Statistical analysis of displacement speed in partially premixed flames using Direct Numerical Simulation

Sean Malkeson[1], Nilanjan Chakraborty[1]

[1]Engineering Department, University of Liverpool,
Brownlow Hill, Liverpool, L69 3GH, United Kingdom

1 Introduction

The propagation statistics plays a key role for modelling of turbulent partially premixed flames [1,2]. Bray *et al.* [2] demonstrated that displacement speed statistics is essential for the Flame surface density (FSD) and level-set based modelling methodology for partially premixed flames. It is possible to define a reaction progress variable c in terms of fuel mass fraction Y_F in the following manner: $c=(\xi Y_{F\infty}-Y_F)/[\xi Y_{F\infty}-\max[0,(\xi-\xi_{st})/(1-\xi_{st})]Y_{F\infty}]$ (where $Y_{F\infty}$ is the fuel mass fraction in the pure fuel stream, ξ is the mixture fraction and ξ_{st} is the stoichiometric mixture fraction) so that c increases monotonically from zero to unity from unburned gases to fully burned products. The speed at which a c isosurface moves normal to itself with respect to an initially coincident material surface is referred to as the displacement speed S_d [2]. The local displacement speed is determined by the balance of reaction and molecular diffusion rates as well as the reactive scalar gradient statistics, which are significantly affected by curvature and strain rate. Although statistical behaviour of S_d have been studied extensively for perfectly premixed flames, relatively less attention is given to S_d statistics in partially premixed flames [2,3]. It is useful to decompose S_d into a number of components (i.e. $S_d = S_r + S_n + S_t + S_\xi$), which are, namely – the reaction rate component S_r , the component due to flame normal molecular diffusion rate S_n, the tangential component S_t and the contribution arising from the reactant inhomogeneity S_ξ . The quantities S_r , S_n , S_t and S_ξ take the following form [2]: $S_r=\dot{\omega}_c/\rho|\nabla c|$, $S_n=\vec{N}.\nabla(\rho D\vec{N}.\nabla c)/\rho|\nabla c|$, $S_t=-2D\kappa_m$ and $S_\xi=A/\rho|\nabla c|$ where $\dot{\omega}_c=-\dot{\omega}_F/\xi Y_{F\infty}$ and $A=-2\rho D\vec{N}.\nabla\xi|\nabla c|/\xi$ for $\xi\le\xi_{st}$, and $\dot{\omega}_c=-\dot{\omega}_F(1-\xi_{st})/\xi_{st}(1-\xi)Y_{F\infty}$ and $A=2\rho D\vec{N}.\nabla\xi|\nabla c|/(1-\xi)$ for $\xi>\xi_{st}$. In the above expressions $\dot{\omega}_c$ is the reaction rate of c, $\vec{N}=-\nabla c/|\nabla c|$ is the local flame normal vector and $\kappa_m=\nabla.\vec{N}/2$ is mean of the local principal curvatures and will henceforth be referred to as curvature in this paper. According to this convention a progress variable c isosurface convex to unburned gas has a positive curvature and vice versa. The objectives of the present study are : (i) to study the statistical behaviour of S_d and it's components in partially premixed flames in terms of their pdfs, (ii) to analyse the local curvature κ_m and tangential strain rate $a_T=(\delta_{ij}-N_iN_j)\partial u_i/\partial x_j$ dependence of local S_d in partially premixed flames.

2 Mathematical background and Numerical implementation

The configuration used earlier by Jimenez *et al*. [4] has been used in this study where species inhomogeneity is introduced in the unburned gas side in the form of sinusoidal equivalence ratio variation ahead of an initially planar laminar premixed flame. Following this, a homogeneous isotropic turbulent velocity field is superimposed on the species distribution and the flame is allowed to interact with turbulence and upstream reactant inhomogeneity. The turbulent fluctuating velocity field is initialised using a pseudo-spectral method following the Batchelor-Townsend energy spectrum. The chemistry is accounted for by a single-step Arrhenius type reaction in which the activation energy and heat of reaction are taken to be functions of equivalence ratio following Tarrazo *et al.* [5] in order to mimic the laminar burning velocity variation with equivalence ratio in hydro-carbon flames. Non-reflecting boundary conditions are used in the direction of the mean flame propagation and the transverse boundaries are taken to be periodic. A 10th order central difference scheme and 3rd order Runge-Kutta method were used for spatial discretisation and time advancement respectively [6]. The initial values of rms turbulent velocity fluctuation normalised by unstrained laminar burning velocity for stoichiometric mixture $u^{/}/S_{L(\varphi=1)}$, integral length scale to flame thickness ratio $\ell S_{L(\varphi=1)}/D_u$, the ratio of wavelength of species inhomogeneity in unburned gas to integral length scale ℓ_φ/ℓ, global mean equivalence ratio $<\varphi>$, equivalence ratio amplitude $\varphi^{/}$, Damköhler number and Karlovitz numbers based on the global equivalence ratio $<\varphi>$ (i.e. $Da(<\phi>) = lS^2_{L(<\phi>)}/u'.D_u$ and $Ka(<\phi>) = [u'/S_{L(<\phi>)}]^{3/2}[l.S_{L(<\phi>)}/D_u]^{-1/2}$) for the cases considered here are listed in Table 1, where D_u is the unburned gas diffusivity and $S_{L\,(<\varphi>)}$ is the laminar burning velocity at global mean equivalence ratio $<\varphi>$. All the cases are run for about two initial eddy turn-over times ($=2\ell/u^{/}$) which is greater than the chemical time scale $D_u/S_{L(\varphi=1)}{}^2$. Simulations are carried out using a uniform grid size of 200x200x200 and domain is taken to be cube of size $28D_u/S_{L(\varphi=1)}$ x $28D_u/S_{L(\varphi=1)}$ x $28D_u/S_{L(\varphi=1)}$. Lewis numbers for all the species are taken to be unity and $(T_{ad}-T_0)/T_0$ is taken to be 3.0 where T_0 and T_{ad} are fresh gas and adiabatic flame temperature of stoichiometric mixture.

Table 1: List of DNS parameters used in the present study

Case	$u'/S_{L(\phi=1)}$	$\ell S_{L(\phi=1)}/D_u$	ℓ_ϕ/ℓ	$Da(<\phi>)$	$Ka(<\phi>)$	$<\phi>$	ϕ'
A	8.0	4.2	10	0.53	10.0	1.0	0.4
B	8.0	4.2	10	0.11	50.0	0.7	0.4

3 Results & Discussion

In order to understand S_d statistics, the variations of the mean values of $\dot{\omega}_c$, $\vec{N}.\nabla(\rho D\vec{N}.\nabla c)$, $(-2\rho D\kappa_m|\nabla c|)$ and A conditional on reaction progress variable c for cases A and B are shown in Figs. 1a and b respectively. It is evident from Figs. 1a and b that the reaction rate attains maximum value close to the burned gas side ($c \approx 0.8$) for both the cases and this location can be considered as the flame location. The mean contribution of $\vec{N}.\nabla(\rho D\vec{N}.\nabla c)$ remains positive towards the fresh gas side and negative towards the burned gas side with a transition close to the middle of the flame brush. This suggests that a negative value of S_d may occur when the negative contributions of $\vec{N}.\nabla(\rho D\vec{N}.\nabla c)$, $(-2\rho D\kappa_m|\nabla c|)$ and A locally overcome the positive semi-definite contribution of $\dot{\omega}_c$. The mean contributions of $(-2\rho D\kappa_m|\nabla c|)$ and A remain negligible compared to the mean values of $\dot{\omega}_c$, and $\vec{N}.\nabla(\rho D\vec{N}.\nabla c)$, for both cases A and B, which is consistent with previous findings of Defransure *et al*. [3]. Comparing Figs. 1a and b it is evident that the mean values of $\dot{\omega}_c$ and $\vec{N}.\nabla(\rho D\vec{N}.\nabla c)$ are smaller in case B than in case A. The variations of $<\dot{\omega}_c + \nabla.(\rho D\nabla c) + A> = <\dot{\omega}_c + \vec{N}.\nabla(\rho D\vec{N}.\nabla c) - 2\rho D\kappa_m|\nabla c| + A>$ and $<\rho_0 S_{L(\phi)}|\nabla c|>$ with c are shown in Figs. 1c and d for cases A and B respectively where <..> signifies ensemble averaging operation on a given c isosurface. Figures 1c and d show that $\dot{\omega}_c + \vec{N}.\nabla(\rho D\vec{N}.\nabla c) - 2\rho D\kappa_m|\nabla c| + A$ remains positive for both cases A and B, which indicates that the surface averaged value of densityweighted displacement speed (i.e. $<\rho S_d>_s = <\rho S_d|\nabla c|>/<\nabla c> = <\dot{\omega}_c + \vec{N}.\nabla(\rho D\vec{N}.\nabla c) - 2\rho D\kappa_m|\nabla c| + A>/<\nabla c>$) remains positive throughout the flame brush. Comparing $<\dot{\omega}_c + \vec{N}.\nabla(\rho D\vec{N}.\nabla c) - 2\rho D\kappa_m|\nabla c| + A>$ and $<\rho_0 S_{L(\phi)}|\nabla c|>$ in Figs. 1c and d it is evident that $<\dot{\omega}_c + \vec{N}.\nabla(\rho D\vec{N}.\nabla c) - 2\rho D\kappa_m|\nabla c| + A>$ remains close to $<\rho_0 S_{L(\phi)}|\nabla c|>$ throughout the flame brush for case A but for case B $<\dot{\omega}_c + \vec{N}.\nabla(\rho D\vec{N}.\nabla c) - 2\rho D\kappa_m|\nabla c| + A>$ is significantly smaller than $<\rho_0 S_{L(\phi)}|\nabla c|>$. In case B combustion situation tends towards the broken reaction zones regime [1] where the reaction-diffusion balance is severely affected by turbulent motion within flame thickness, which along with significant flame thinning results in a smaller value of $<\dot{\omega}_c + \vec{N}.\nabla(\rho D\vec{N}.\nabla c) - 2\rho D\kappa_m|\nabla c| + A>$ than $<\rho_0 S_{L(\phi)}|\nabla c|>$.

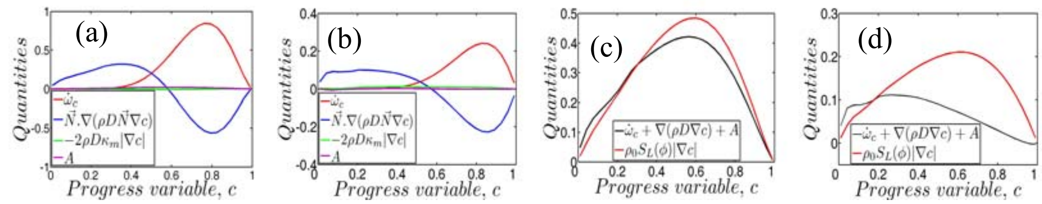

Fig1: The mean variations of $\dot{\omega}_c, \vec{N}.\nabla(\rho D\vec{N}.\nabla c), (-2\rho D\kappa_m|\nabla c|)$ and A with c across the flame brush: (a) case A, (b) case B. The variations of $<\dot{\omega}_c + \nabla.(\rho D\nabla c) + A>$ and $<\rho_0 S_{L(\phi)}|\nabla c|>$ with c across the flame brush for (c) case A, (d) case B. The quantities are normalised by $D_u/S_{L(\varphi=1)}{}^2$.

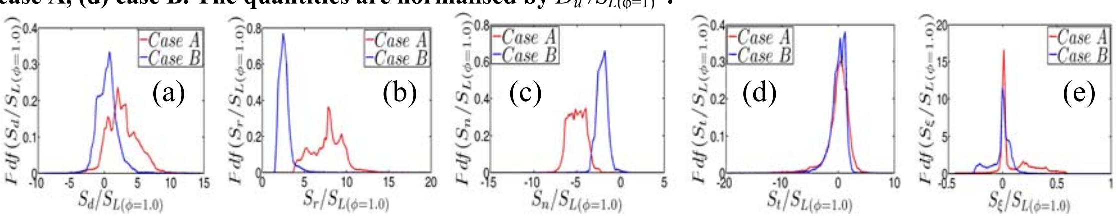

Fig. 2: Pdfs of (a) $S_d/S_{L(\varphi=1)}$, (b) $S_r/S_{L(\varphi=1)}$, (c) $S_n/S_{L(\varphi=1)}$, (d) $S_t/S_{L(\varphi=1)}$ and (e) $S_\xi/S_{L(\varphi=1)}$ at c = 0.8 isosurface for cases A and B.

The pdfs of $S_d/S_{L(\varphi=1)}$, $S_r/S_{L(\varphi=1)}$, $S_n/S_{L(\varphi=1)}$, $S_t/S_{L(\varphi=1)}$ and $S_\xi/S_{L(\varphi=1)}$ for a c isosurface close to the maximum reaction rate ($c \approx 0.8$) are shown in Figs.2a-e for both cases A and B. It can be observed from Fig. 2a that there are non-zero probabilities of finding negative values of S_d for both cases A and B but the probability of finding positive values supersede that of finding negative values and the mean value of S_d remains positive for both the cases. Figure 2a suggests that the probability of finding positive (negative) value of S_d is greater (smaller) in case A and the most probable value of S_d in case A is also found to be greater than that in case B. Figures 2b and c indicate that the probabilities of finding high positive and negative values of $S_r/S_{L(\varphi=1)}$ and $S_n/S_{L(\varphi=1)}$ respectively are greater in case A than those in case B, However, the pdfs of $S_t/S_{L(\varphi=1)}$ do not to differ greatly for both cases where the probabilities for finding both positive and negative values are roughly equally likely and the peak of the pdf is attained at $S_t/S_{L(\varphi=1)} \approx 0$ as the flames are statistically planar in nature. The component $S_\xi/S_{L(\varphi=1)}$ for both cases is shown to be negligible with a value of $S_\xi \approx 0$ being most likely. From Figs. 2a-e it can be seen that the maximum magnitude of S_ξ remains negligible compared to the magnitudes of S_r, S_n, and S_t. The most significant effect on the behaviour of displacement speed originates from (S_r+S_n+S_t). The contours of joint pdf between S_d and κ_m for case A are shown in Fig. 3a at c = 0.8 isosurface which exhibits a negative correlation. The same qualitative behaviour has been observed in case B. As S_t is by definition deterministically negatively correlated with curvature it is useful to analyse the correlation between (S_r+S_n) and κ_m, which is presented in Fig. 3b for case A. Figure 3b shows a weak correlation between (S_r+S_n) and κ_m which indicates that the negative correlation between S_t and κ_m is principally responsible for a net negative correlation between S_d and κ_m in case A. The same qualitative behaviour has also been observed in case B. For both cases A and B, S_d is weakly correlated with tangential strain rate a_T, which is evident for case A from Fig. 3c. However, (S_r+S_n) shows a negative correlation with tangential strain rate a_T which is shown for case A in Fig. 3d and the same behaviour is observed in case B. Figure 3e demonstrates that a_T and κ_m are negatively correlated, which also holds qualitatively in case B. This negative correlation between a_T and κ_m leads to a positive correlation between S_t and a_T, which opposes the negative correlation between (S_r+S_n) and a_T and leads to a weak correlation between S_d and a_T for both cases A and B. The curvature and strain rate dependence of S_d is found to be consistent with earlier findings in the context of perfectly premixed flames [6]. The local strain rate and curvature dependence of S_d needs to be accounted for both FSD and level-set method based reaction rate closure to turbulent partially premixed combustion.

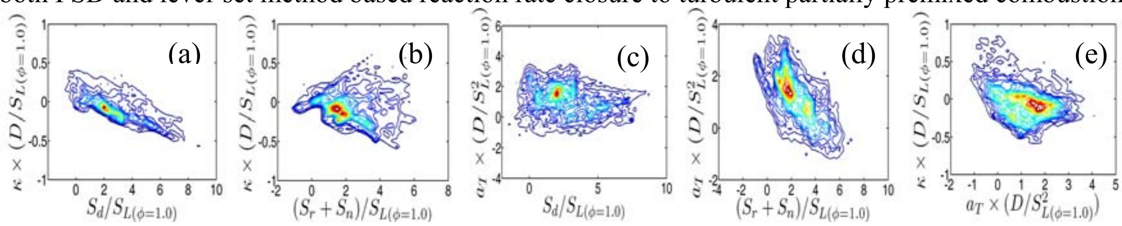

Fig. 3: Contours of joint pdfs (a) S_d-κ_m, (b) (S_r+S_n)-κ_m, (c) S_d-a_T, (d) (S_r+S_n)-a_T and (e) a_T-κ_m at c =0.8 isosurface for case A with blue and red indicating low and high probability regions respectively.

4 Conclusions

The statistics of S_d for globally fuel-lean and stoichiometric (i.e. $\langle\varphi\rangle$=0.7 and 1.0) partially premixed flames have been studied using 3D compressible DNS data. It has been found that the magnitude of the component of displacement speed due to reactant inhomogeneity S_ξ remains negligible in comparison to the magnitudes of S_r , S_n and S_t. The pdfs of S_d show probabilities of finding negative values but the probability of finding positive values overcome that of finding negative values to result in a net positive mean value of S_d. The local displacement speed S_d is found to be negatively correlated with curvature κ_m , principally due to negative S_t-κ_m correlation. The negative correlation between a_T and κ_m gives rise to a positive correlation between S_t and a_T which opposes the negative correlation between (S_r+S_n) and a_T to yield a weak S_d-a_T correlation. These strain rate and curvature dependence of S_d are required to be taken into account while modelling turbulent partially premixed flames using both FSD and level-set methods of reaction rate closure.

References

[1] Peters,N. (2000) Turbulent Combustion, 1st Ed, Cambridge University Press, U.K.

[2] Bray, K. et al. (2005) Role of the progress variable in models for partially premixed turbulent combustion, Combust. Flame, 141:431.

[3] Defransure, F. et al. (2003) Experimental and numerical studies of the laminar flame speed of stratified flames, Proceedings of 1st European Combustion Meeting, Orleans, France.

[4] Jimenez, C. et al. (2002) Numerical simulation and modeling for lean stratified propane-air flames, *Combust. Flame*, 128:1.

[5] Tarrazo, E. et al. (2006). A simple one-step chemistry model for partially premixed hydrocarbon combustion,Combust. Flame, 147:32.

[6] Chakraborty, N., Cant, S.(2004) Unsteady effects of strain rate and curvature on turbulent premixed flames in an inflow–outflow configuration, *Combust. Flame*, 137:129.